Chinese Chemical Letters 37 (2026) 111928

Contents lists available at ScienceDirect

Chinese Chemical Letters

journal homepage: www.elsevier.com/locate/cclet

# Electrochemical selenylation of tyrosine oligopeptides to benzo[*b*]furan-functionalized peptides

Xinwei Hu[a,1], Yong Zeng[a,1], Jiongdong Ma[a,1], Han Diao[a,1], Fei-Xiao Chen[b], Mu Chen[a], Shou-Kun Zhang[a], Chengzhi Jin[a,*], Shao-Fei Ni[b,*], Zhixiong Ruan[a,*]

[a] *Department of Guangzhou Municipal and Guangdong Provincial Key Laboratory of Molecular Target & Clinical Pharmacology and the State Key Laboratory of Respiratory Disease, School of Pharmaceutical Sciences, Guangzhou Medical University, Guangzhou 511436, China*
[b] *Department of Chemistry and Key Laboratory for Preparation and Application of Ordered Structural Materials of Guangdong, Shantou University, Shantou 515063, China*

ARTICLE INFO

*Article history:*
Received 2 September 2025
Revised 24 September 2025
Accepted 29 September 2025
Available online 1 October 2025

*Keywords:*
Electrochemical
Tyrosine oligopeptides
Selenylation
Benzo[*b*]furan
Biocompatibility

ABSTRACT

Benzo[*b*]furans are significant scaffolds in drug molecules and are prevalent structural components in natural products. Chemically encoded non-natural peptidomimetics have a substantial impact on pharmaceuticals by offering enhanced stability, improved cell permeability, and resistance to enzymatic degradation. Consequently, a strategy for the sustainable assembly of benzo[*b*]furan/benzopyran-functionalized peptides through the electrochemical late-stage modification of alkyne-modified tyrosine oligopeptides is proposed. This approach facilitates the multifunctional integration of non-native tyrosine-derived substrates, as well as their subsequent functionalization. Notably, the resulting peptides exhibit favorable properties regarding biocompatibility and cellular uptake.

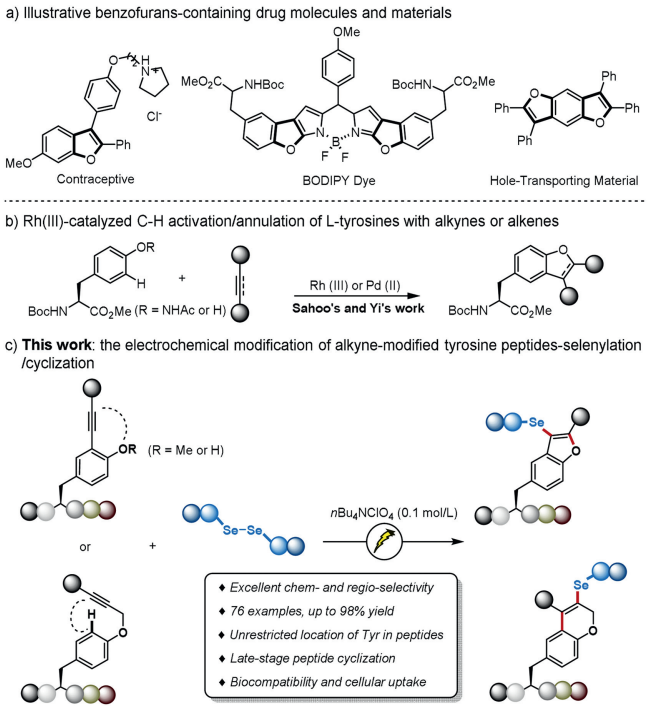
© 2025 Published by Elsevier B.V. on behalf of Chinese Chemical Society and Institute of Materia Medica, Chinese Academy of Medical Sciences.

The benzo[*b*]furan nucleus serves as a fundamental building block for numerous pharmaceuticals [1] and dyes [2,3] due to its significant biological activity and electronic transmission properties (Scheme 1a). In recent years, the cyclization of tyrosines featuring a benzo[*b*]furan skeleton [4–8], catalyzed by transition metals, has been reported (Scheme 1b). Among the methods for directly constructing the benzo[*b*]furan skeleton [9,10], those that utilize transition metals offer an attractive opportunity for sustainable peptide modification of tyrosines, owing to their versatility and cost-effectiveness. The appeal of phenolic derivatives in protein modification [11,12] and drug development, along with the prominent role of selenium-containing compounds [13,14] in peptide drugs, underscores the desirability of direct cyclization and selenization of tyrosine derivatives as a strategy for amino acid modifications [15]. Over the past decade, significant efforts have been made to enhance the functionalization of the aromatic ring in tyrosine using complexes of iron [16,17], palladium [18–23], nickel [24], rhodium [25,26], ruthenium [27,28], and others [29,30]. Despite this undeniable progress, chemical oxidants are often required to achieve specific stoichiometries, leading to undesirable waste products and metal residues that compromise overall atom economy and green synthesis pathways. In light of this, new synthetic methods such as photocatalysis [31–37], electrochemical synthesis [38–42], and enzyme catalysis [43] have emerged to address the limitations of metal-catalyzed-cyclization. However, there remains a lack of diverse synthetic approaches for tyrosine peptide reactions that incorporate unique skeletons and functional groups.

In the current context of green synthesis, the integration of amino acid modification and electrochemical synthesis has recently been recognized as a particularly powerful tool for molecular catalysis [44–47]. This approach helps to eliminate the needfor stoichiometric chemical oxidants while facilitating the regioselective synthesis of peptides. Despite the undeniable advancements in electrochemical synthesis [48–54], the recent diversification of amino acids or peptides containing benzofuran structures remains infrequently reported. Based on our research progress in the electrochemical modification of peptides [55–58], we herein disclosed the first electrochemically selective cyclization and selenylation of alkyne-modified *O*-methyltyrosine oligopeptides with diaryl selenides for late-stage tyrosine modifications (Scheme 1c). Notable features of this strategy include: (1) Excellent regioselectivity and high tolerance to functional groups, enabling the late cyclization of peptides and yields of up to 98%; (2) unrestricted position of the tyrosine in the peptides; (3) electrochemical reduction for late-stage diversification of alkyne-modified *O*-methyltyrosine oligopep-

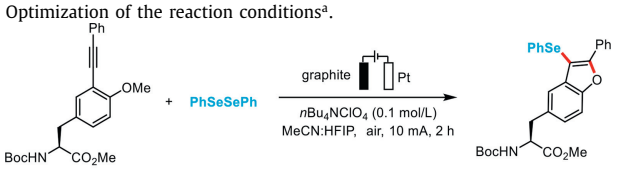
* Corresponding authors.
*E-mail addresses:* chengzhijin@gzhmu.edu.cn (C. Jin), sfni@stu.edu.cn (S.-F. Ni), zruan@gzhmu.edu.cn (Z. Ruan).
[1] These authors contributed equally to this work.

https://doi.org/10.1016/j.cclet.2025.111928
1001-8417/© 2025 Published by Elsevier B.V. on behalf of Chinese Chemical Society and Institute of Materia Medica, Chinese Academy of Medical Sciences.




**Scheme 1.** Research progress on the reaction of tyrosine cyclization to construct benzofuran/benzopyran derivatives.

**Table 1**
Optimization of the reaction conditions[a].



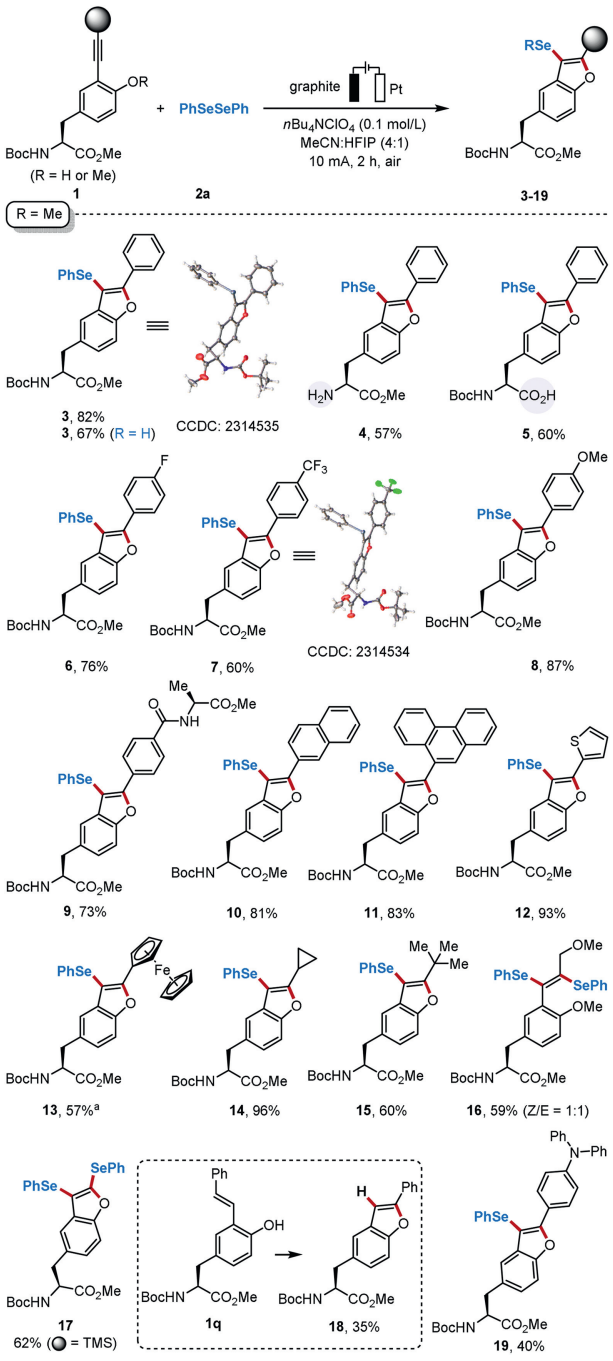

1a 2a 3

| Entry | Deviation from standard conditions | Yield (%)[b] |
|---|---|---|
| 1 | None | 82 |
| 2 | No current | 0 |
| 3 | No $n$Bu$_4$NClO$_4$ | 0 |
| 4 | $n$-Bu$_4$NHSO$_4$ instead of $n$Bu$_4$NClO$_4$ | 35 |
| 5 | $n$-Bu$_4$NI instead of $n$Bu$_4$NClO$_4$ | Trace |
| 6 | $n$-Bu$_4$NPF$_6$ instead of $n$Bu$_4$NClO$_4$ | 65 |
| 7 | MeCN as solvent | 67 |
| 8 | HFIP as solvent | 52 |
| 9 | MeOH as solvent | 42 |
| 10 | MeCN/HFIP (1:1) | 63 |
| 11 | MeCN/HFIP (1:4) | 58 |
| 12 | MeCN/H$_2$O (3:2) | 77[c] |
| 13 | MeCN/Buffer (3:2) (PBS, 0.01 mol/L, pH 7.4) | 77[c] |
| 14 | Current = 40 mA | 80 |
| 15 | Graphite instead of Pt as cathode | 66 |

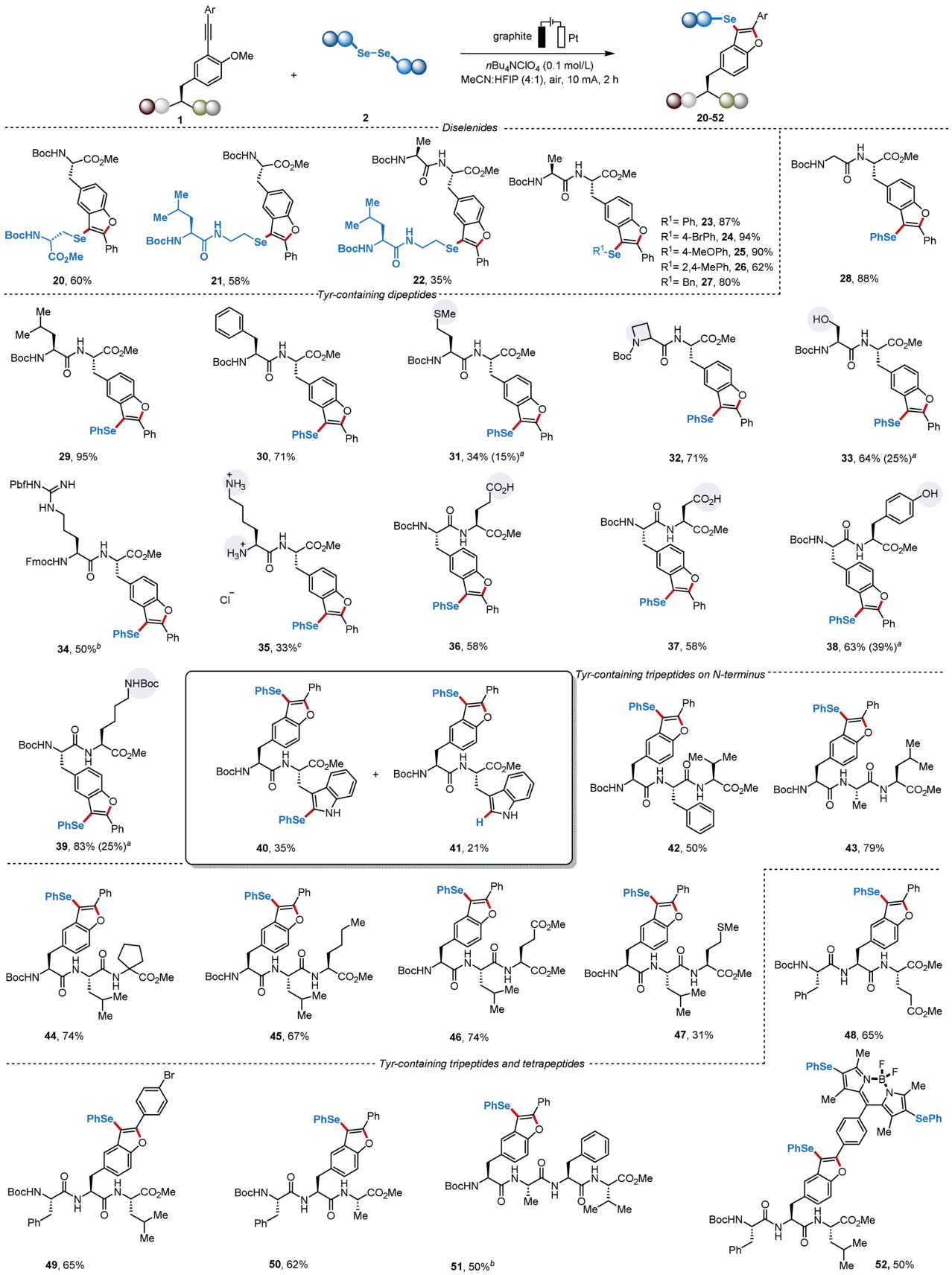
[a] Reaction conditions: Undivided cell, graphite anode (1.0 cm × 1.0 cm × 0.2 cm), Pt cathode (1.0 cm × 1.0 cm × 0.01 cm), **1a** (0.3 mmol), **2a** (0.36 mmol), $n$-Bu$_4$NClO$_4$ (1.0 mmol), MeCN: HFIP = 4:1 (10 mL), constant current = 10 mA, 2.0 h (2.5 F/mol), r.t., under air.
[b] Yields of isolated products.
[c] 10 h.

tides; and (4) the modified tyrosine-derived peptides exhibit favorable outcomes regarding biocompatibility and cellular uptake.

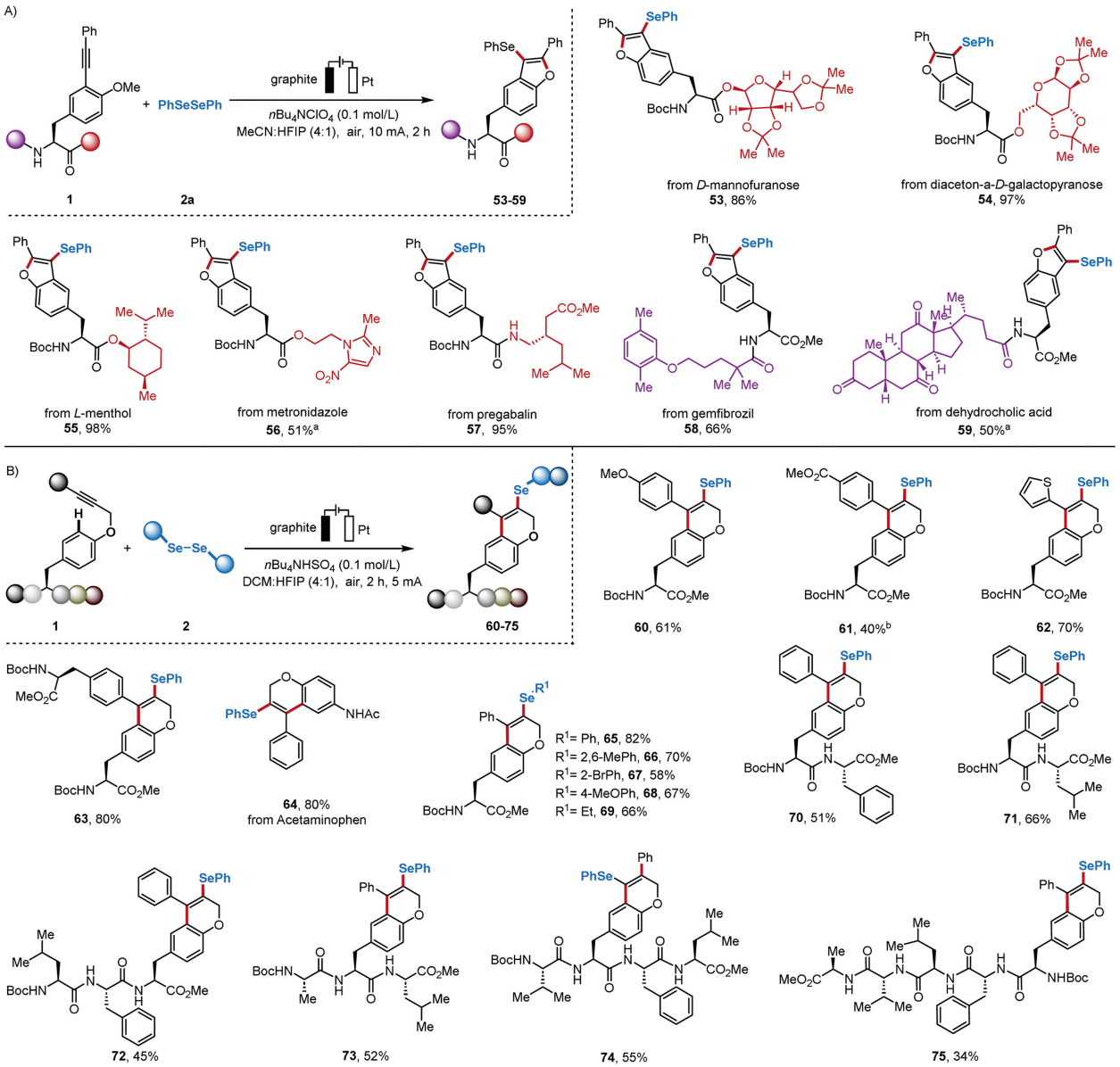
An extensive screening of conditions was conducted using methyl (*S*)-2-((*tert*–butoxycarbonyl)amino)-3-(4–methoxy-3-(phenylethynyl)phenyl)propanoate (**1a**) and diphenyl diselenide (**2a**) as model substrates in a simple undivided cell setup, which employed a graphite anode and a platinum plate (Pt) cathode (Table 1 and Tables S1 and S2 in Supporting information). Compound **3** was obtained in 82% yield when the commonly used substrates **1a** and **2a** were directly electrolyzed at a constant current of 10 mA in a mixed electrolyte solution of $n$Bu$_4$NClO$_4$ in MeCN/HFIP (4:1) at room temperature under atmospheric conditions (Table 1, entry 1). Further control experiments confirmed the critical role of external current and electrolyte composition (Table 1, entries 2 and 3). Altering the anion of the electrolyte resulted in a significant decrease in yield (Table 1, entries 4–6). Similarly, the use of MeCN, whether as the sole solvent (Table 1, entries 7–9) or as a co-solvent, proved essential for product formation. However, changing the ratio of MeCN to HFIP led to a slight but noticeable decline in reaction efficiency (Table 1, entries 10 and 11). Notably, replacing HFIP with H$_2$O or buffer still afforded the target product




**Scheme 2.** Scope of the late-stage functionalization of alkyne-modified tyrosines. [a] 8 h (10.0 F/mol).




**Scheme 3.** Scope of the late-stage functionalization of Tyr-containing oligopeptides. Isolated yields are reported. [a] $H_2O$ instead of HFIP. [b] $nBu_4NHSO_4$ (0.1 mol/L) instead of $nBu_4NClO_4$ (0.1 mol/L). [c] After the reaction completed, 1 mL of HCl (2 mol/L) was added.



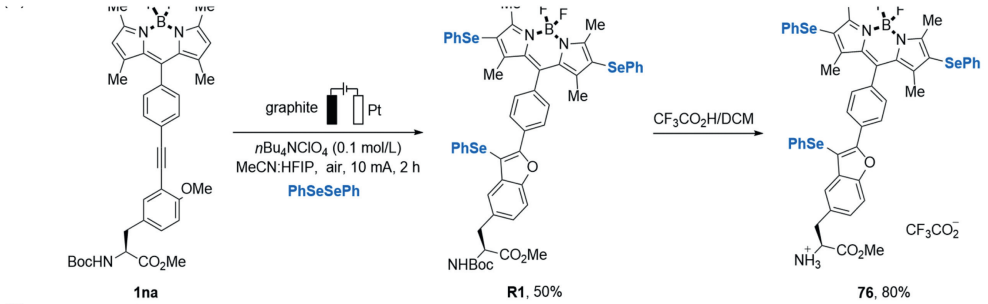

**Scheme 4.** (A) Late-stage functionalization *via* electrochemical selenylation of alkyne-modified tyrosine peptides. (B) Scope of constructing benzopyran derivatives using alkyne-modified tyrosine oligopeptides. Isolated yields are reported. [a] $n$Bu$_4$NHSO$_4$ (0.1 mol/L) instead of $n$Bu$_4$NClO$_4$ (0.1 mol/L). [b] 4 h (2.5 F/mol).

**3** in good yield upon extending the reaction time (Table 1, entries 12 and 13).

Furthermore, increasing the current to 40 mA showed no significant effect on the yield (Table 1, entry 14). The critical role of platinum as an efficient electron transport material was demonstrated when a graphite sheet was used in place of platinum as the cathode material (Table 1, entry 15).

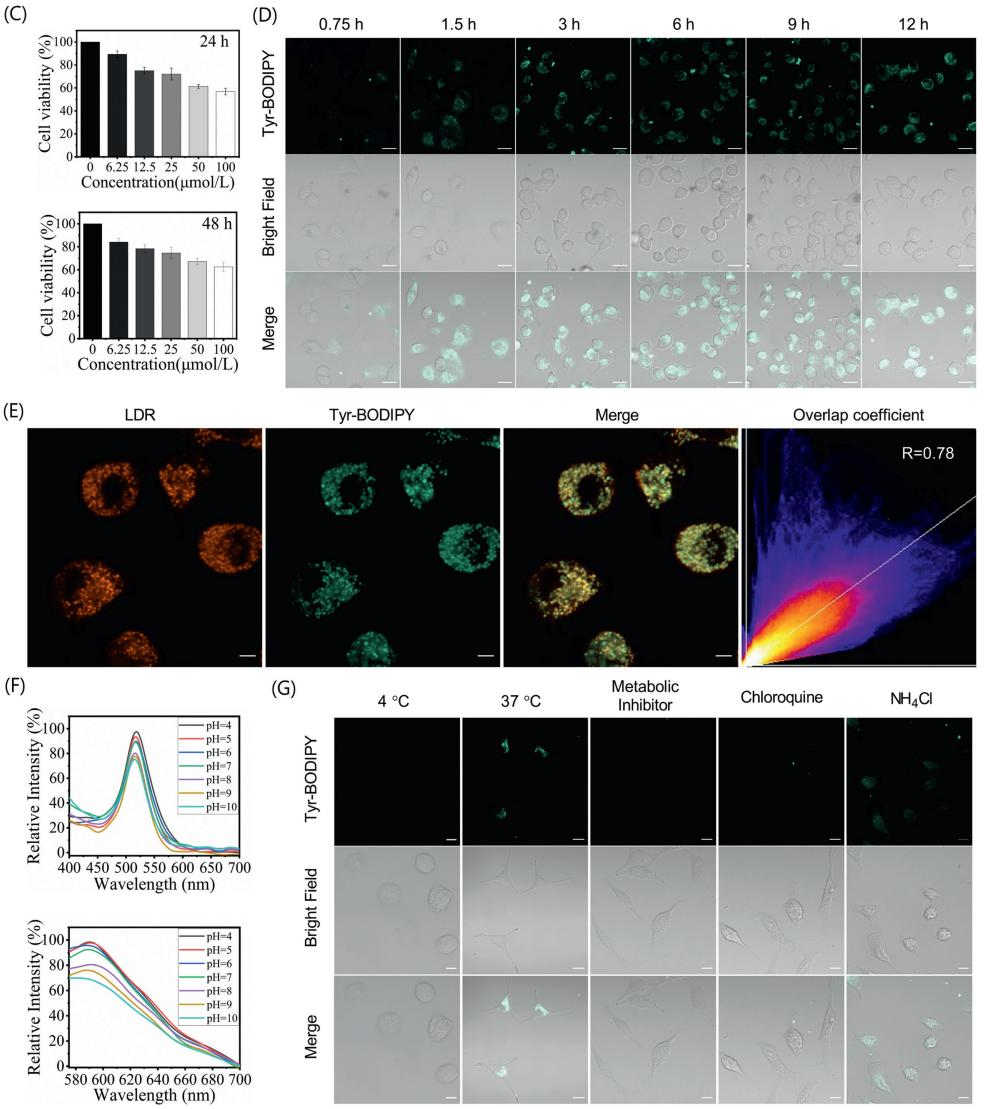
Having established optimal reaction conditions, we investigated the substrate scope of various alkyne-modified *O*-methyltyrosines for cyclization with diphenyl diselenides (**2a**) (Scheme 2). The protocol proved suitable for the use of 2-alkynyl tyrosine (**1b**), yielding the desired benzo[*b*]furan tyrosines (**3**) in 67 % yield. The exact structures of compounds **3** (CCDC: 2314535) and **7** (CCDC: 2314534) were further confirmed by X-ray analysis. Surprisingly, the unprotected amino (**4**) or carboxyl groups (**5**) were still able to give the product without oxidation in this system. Electron-withdrawing (-F, -$CF_3$, -Ala) and electron-donating (-OMe) groups at the *para* position underwent smooth conversion to afford the selenylation products (**6**–**9**) in good to excellent yields. In addition to the various electronic substituents on the aromatic ring, polycyclic aromatic (naphthalene, anthracene) and heteroaryl (thiophene, ferrocene) alkyne-substituted tyrosines were also well tolerated, resulting in cyclization products **10**–**13**. Notably, the cyclopropane-substituted alkynyl tyrosine was selected to produce the selenium-substituted cyclization product (**14**) with high selectivity and near-equivalent yields, rather than the ternary ring-opening product. Furthermore, aliphatic alkynes were also compatible, leading to the corresponding selenylation tyrosines (**14**–**16**) with moderate conversions, while the trimethylsilyl groups (**17**) maintained good reactivity. Surprisingly, the scope of tyrosines for this protocol could be readily extended to include vinyl (**18**). Not only that, triphenylamine (**19**) are also well adapted to the reaction system in moderate yields.

Considering the unique advantages and latent potential of selenylation modifications in peptides, and based on our recent research interest in electrochemical peptides, we selected various types of diselenides and alkyne-modified tyrosine oligopeptides to explore new potentially pharmaceutically active tyrosine deriva-



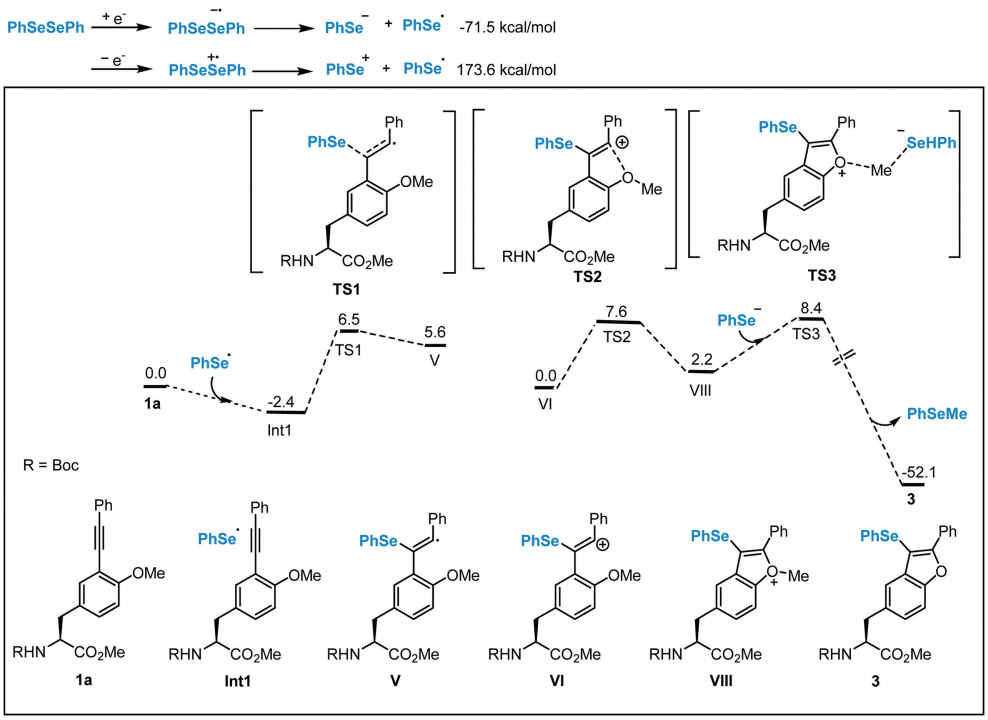

(B)

| | $\Lambda_{abs}$ (nm) | ε ($cm^{-1}\cdot M^{-1}$) | $\Lambda_{em}$ (nm) | Stokes shift ($cm^{-1}$) | $\Phi_{FL}$ | $\Phi\,^1O_2$ |
|---|---|---|---|---|---|---|
| Tyr-BODIPY | 516 nm | 46900 | 591 nm | 2459 | 0.20 | 0.23 |




**Scheme 5.** The bioactivity exploration of Tyr-BODIPY (**76**). A) Preparation of Tyr-BODIPY. (B) Photophysical data of Tyr-BODIPY in methanol solution. (C) MTT assay of Tyr-BODIPY. (D) Confocal images of Tyr-BODIPY with extended incubation time. (E) Confocal imaging of Tyr-BODIPY and lyso racker deep red. (F) UV–vis and luminescence spectrum of Tyr-BODIPY in the range pH 4–10. (G) Uptake mechanism of Tyr-BODIPY. Tyr-BODIPY, $\lambda_{ex}$, 488 nm, $\lambda_{em}$, 545–595 nm; for LysoTracker Deep Red, $\lambda_{ex}$, 631 nm, $\lambda_{em}$, 650–700 nm. Scale bar: 20 μm.

tives through the cyclization of selenides (Scheme 3). As shown, the selenium-substituted amino acids appeared to be quite compatible and delivered peptide derivatives (**20**–**22**) when compared with commercially available diselenides building blocks. Furthermore, a wide range of aryl and alkyl diselenides could be successfully incorporated into the phenolic motif of Tyr residues, resulting in the benzo[*b*]furan tyrosine products **23**–**27** with excellent yields. Notably, dipeptides bearing Gly, Leu, Phe, Met, Ser, Arg, Lys, and Trp at the C-terminus performed well under standard conditions, providing the corresponding products with moderate to excellent



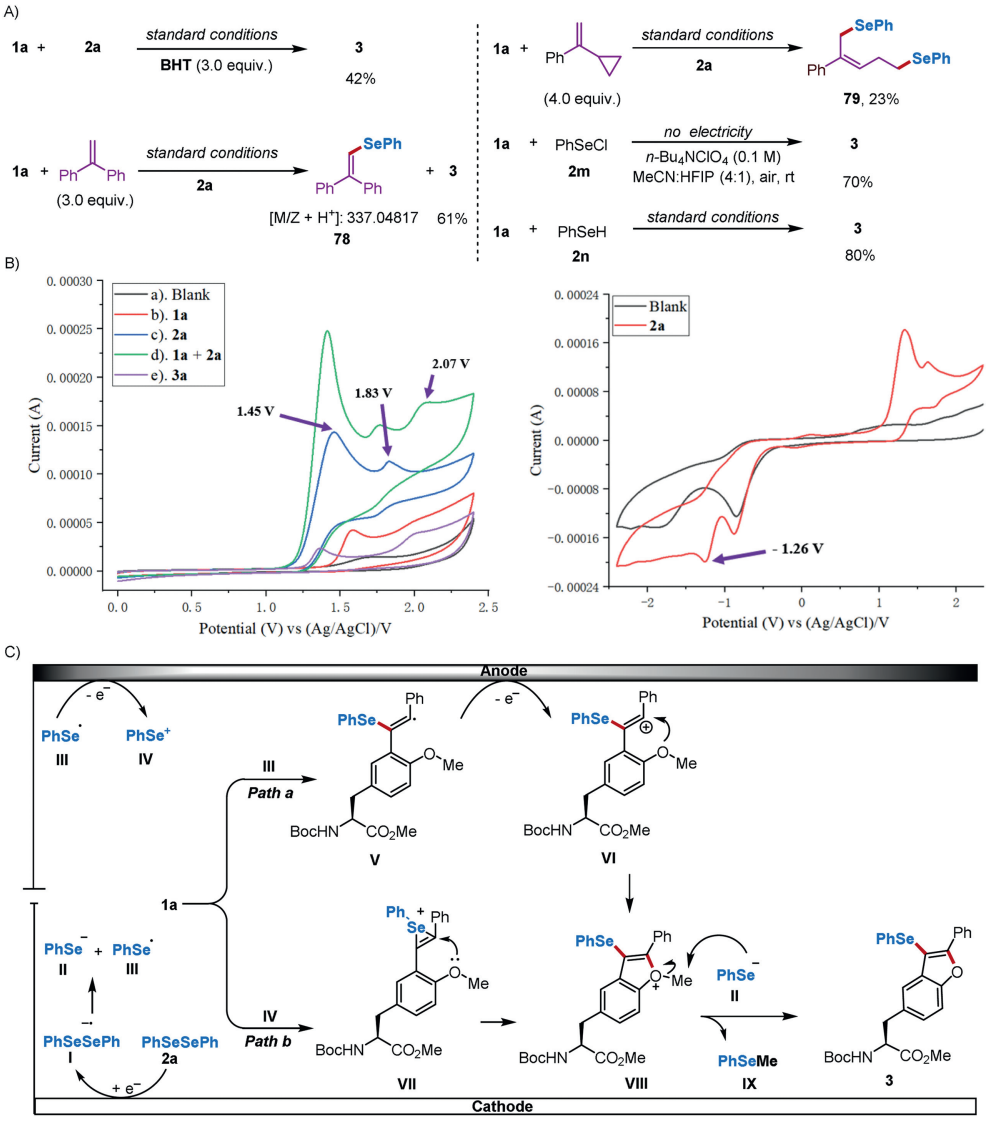

**Scheme 6.** DFT-calculated potential energy surface of **1a**'s conversion process. All energy units are kcal/mol.

yields (**28**–**35**). Moreover, tripeptides containing Tyr residues at the *N*-terminus could also be effectively functionalized, yielding products **42**–**47**, although there was a significant decrease in yield with Met. Surprisingly, we were pleased to discover that the cyclization of Tyr-containing peptides with non-specific positions was also successful using this protocol, affording the modified tripeptides and tetrapeptides **48**–**51**. Even when bearing the biocompatible fluorescent BODIPY group, the target product **52** was obtained in moderate yields.

We next evaluated the capacity of alkyne-modified tyrosine selenium cyclization to directly construct benzo[*b*]furan tyrosine-bearing pharmaceuticals (Scheme 4A). High-yield tyrosine ester derivatives were obtained through an electrochemical method using commercial D-manfuranose, diaceton-$\alpha$-D-galactopyranose, L-menthol, and metronidazole (**53**–**56**). Additionally, a variety of commercially available drugs and derivatives with furan structures, such as pregabalin, gemfibrozil (Lopid) and dehydrocholic acid (**57**–**59**), can be effectively electrochemically functionalized using diaryl selenides to produce novel, undisclosed peptide analogs. Overall, the reaction was very clean, with no byproducts observed; however, complete conversion was not always achieved, and $n$Bu$_4$NClO$_4$ was occasionally substituted with $n$Bu$_4$NHSO$_4$.

Inspired by the success of cross-coupling reactions involving alkyne-modified tyrosines and diphenyl diselenides, we shifted our focus to non-activated alkynes to synthesize selenated benzopyrans, which are challenging to isolate and serve as intermediates in various reactions (Scheme 4B). Under these modified conditions, **2a** was readily coupled with tyrosines possessing electron-donating (-OMe), electron-withdrawing (-$CO_2$Me), and heterocyclic substituents on the phenyl ring, providing the corresponding benzopyran-incorporated tyrosine derivatives **60**–**63**. Notably, further investigation revealed that acetaminophen also served as a suitable reactant for the coupling with diphenyl diselenides, affording the desired seleno-benzopyran derivatives (**64**) incorporating a pharmaceutical scaffold. Subsequently, our attention was turned to various commercially available diselenides. Coupling of tyrosine with different aryl or alkyl diselenides furnished the target products **65**–**69**. Furthermore, tyrosine-containing dipeptides (**70** and **71**), tripeptides (**72** and **73**), tetrapeptides (**74**), and pentapeptides (**75**) smoothly underwent the developed selenocyclization, yielding the desired products in moderate yields regardless of the specific tyrosine position within the peptide chain. This observation highlights the significant potential of this protocol for constructing peptide-integrated architectures.

To further assess the biological application potential of this compound series, compound **76** (Scheme 5A), a selenotyrosine-conjugated fluorescent probe with favorable photophysical properties, was selected for initial investigation of cellular uptake and bioimaging (Scheme 5 and Figs. S2-S10 in Supporting information). The biocompatibility of the compound was assessed using the MTT assay, a standard method for measuring cell viability. To avoid the influence of the absorption of the compound, the absorption value at a wavelength of 600 nm was recorded. The results indicated no significant cytotoxic effects on A549 cells, with $IC_{50}$ values exceeding 100 μmol/L after 24 or 48 h of incubation (Scheme 5C). Furthermore, through the optimization of cell culture conditions, the fluorescence signal of the compound showed no obvious change after a 3-h incubation, indicating that the uptake equilibrium time of the compound in A549 cells was approximately 3 h (Scheme 5D). Moreover, experimental evidence on phototoxicity and biostability demonstrates that compound **76** has no significant impact on the imaging studies performed in this work (Figs. S7 and S10). The co-staining experiment with a commercial dye (Lysotracker Deep Red, LDR) revealed favorable co-localization between Tyr-BODIPY and LDR. These results indicated a specific lysosomal distribution within A549 cells, highlighting the compound's potential for precise subcellular organelle aggregation (Scheme 5E). To confirm this phenomenon, physiological pH-dependent photoluminescence fluctuations were considered. The results indicated that under neutral to acidic conditions (pH 4–7), the fluorescence signal exhibited only a modest change (<10 %), whereas in the corresponding neutral to alkaline environment (pH 7–10), the fluorescence signal variation was somewhat greater (~20 %) (Scheme 5F). This could be attributed to the formation of ionic compounds under alkaline




**Scheme 7.** Proposed reaction mechanism. (A) Preliminary mechanism studies. (B) Cyclic voltammograms. Conditions: a glassy carbon working electrode, a Ag/AgCl (3 mol/L KCl) reference electrode, and a platinum wire counter electrode, 0.01 mol/L analyte in 0.1 mol/L $n$Bu$_4$NClO$_4$ dissolved in MeCN:HFIP (4:1), 100 mV/s scan rate. (C) Possible mechanism.

conditions. Energy inhibition and partial endocytosis inhibitors significantly reduced the compound's fluorescence signal, implicating energy-dependent endocytic pathways in cellular internalization, a common mechanism for nanoparticle uptake (Scheme 5G). Considering the similarities among molecules in this series, it is likely that similar molecules may utilize energy-dependent endocytosis for localization within lysosomes. These preliminary results can guide the expansion of molecular libraries and further exploration into biological applications.

As illustrated in Scheme 6, the reaction mechanism initiates with the cathodic reduction of diselenide, exothermically generating a selenium radical and a selenide anion. The selenium radical then undergoes addition to alkyne **1a** through transition state **TS1** with an activation barrier of 8.9 kcal/mol, forming intermediate **V**. Subsequently, **V** is anodically oxidized to generate carbocation **VI**, which undergoes cyclization *via* transition state **TS2** with an activation barrier of 7.6 kcal/mol, affording carbocation intermediate **VIII**. Finally, **VIII** reacts with the selenide anion ($PhSe^-$) through transition state **TS3** with an activation barrier of 6.2 kcal/mol, yielding the cyclic selenium product **3** and releasing PhSeMe. This final step is accompanied by significant heat evolution, consistent with the exothermic nature of the overall process.

To gain further mechanistic insights, control experiments were conducted (Scheme 7A). The reaction of **1a** with **2a** was significantly inhibited in the presence of a radical scavenger, such as BHT. Subsequently, the existence of phenylselenyl radicals was corroborated through electrochemical radical trapping experiments, wherein aryl alkenes were employed as radical traps to detect products **78** and **79**. additional studies revealed that **1a** could afford the desired product **3** in 70 % yield under electrochemical conditions in the presence of **2m**, whereas no reaction occurred in the absence of current. Notably, when **2a** was replaced by **2n** under standard conditions, product **3** was still obtained in moderate to good yield, confirming that the reaction proceeds *via* a selenonium ion pathway. Furthermore, as shown in Scheme 7b, cyclic voltammetry (CV) experiments were conducted to investigate the redox potential of the substrate. It was found that **2a** undergoes reduction (−1.26 V) and oxidation (1.45 V and 1.83 V). This indicates that **2a** undergoes a cycle involving one reduction and two oxidations and is preferentially reduced at the cathode. Further testing of a mixture of **1a** and **2a** revealed a new oxidation peak at 2.07 V. This peak can be attributed to the oxidation of the alkenyl radical, supporting the **TS1**–**TS2** process identified in the DFT calculations.

Based on DFT calculations and the mechanistic insights discussed above, a possible mechanism for the selenocyclization *via* electrochemical reduction of alkyne-modified tyrosine is proposed in Scheme 7C. The reaction may be initiated by the formation of seleno radical **III** and selenium anion **II** through cathodic reduction (Schemes 6, 7B and C). Subsequently, the addition of radical **III** to the alkyne generates alkenyl radical **V** with good regioselectivity *via* pathway a. This process is followed by further oxidation and cyclization to form **VIII**, accompanied by the release of PhSeMe (detected by NMR), resulting in the product **3**. Alternatively, we cannot rule out pathway b, in which **III** undergoes anodic oxidation to form selenium cation **IV**, which then reacts with **1a** to create the cyclic selenium intermediate **VII**. This is followed by further cyclization to form **VIII**, which subsequently reacts with phenyl selenium anions to yield the final product **3**.

In summary, we have developed an electrochemical method for the selenium cyclization of 2-alkynyl tyrosines with diselenides for direct construction of the benzo[*b*]furan/benzopyran tyrosine derivatives with high chemo- and site-selectivity. Notably, this catalytic system operates independently of tyrosine position within peptide chains. Mechanistically, DFT calculations corroborated the involvement of a selenium radical pathway. Furthermore, the developed protocol allows direct integration of pharmaceutical motifs into peptide architectures, thereby facilitating the modification and utilization of structurally diverse alkyne-modified tyrosine derivatives. Studies on cellular uptake of peptide-conjugated fluorescent compounds underscore their potential for further bioactivity evaluation.

## Declaration of competing interest

The authors declare that they have no known competing financial interests or personal relationships that could have appeared to influence the work reported in this paper.

## CRediT authorship contribution statement

**Xinwei Hu:** Writing – original draft, Project administration, Funding acquisition, Data curation, Conceptualization. **Yong Zeng:** Writing – original draft, Investigation, Data curation, Conceptualization. **Jiongdong Ma:** Validation, Investigation, Data curation. **Han Diao:** Formal analysis, Data curation. **Fei-Xiao Chen:** Validation, Software. **Mu Chen:** Validation, Formal analysis. **Shou-Kun Zhang:** Validation, Formal analysis. **Chengzhi Jin:** Writing – review & editing, Funding acquisition, Formal analysis. **Shao-Fei Ni:** Validation, Software. **Zhixiong Ruan:** Writing – review & editing, Writing – original draft, Supervision, Funding acquisition, Conceptualization.

## Acknowledgments

Support by the National Natural Science Foundation of China (Nos. 22271067, 22201052), Guangzhou Science and Technology Project (No. 2024A04J3036), Open Research Fund of Songshan Lake Materials Laboratory (No. 2023SLABFN23), and the Plan on Enhancing Scientific Research in Guangzhou Medical University (GMU) is most gratefully acknowledged.

## Supplementary materials

Supplementary material associated with this article can be found, in the online version, at doi:10.1016/j.cclet.2025.111928.

## References

[1] P. Cagniant, D. Cagniant, Adv. Heterocycl. Chem. 18 (1975) 337–482.
[2] J.L. Belmonte-Vázquez, E. Avellanal-Zaballa, E. Enríquez-Palacios, et al., J. Org. Chem. 84 (2019) 2523–2541.
[3] H. Tsuji, C. Mitsui, L. Ilies, Y. Sato, E. Nakamura, J. Am. Chem. Soc. 129 (2007) 11902–11903.
[4] H. Chen, H.C.F. Wong, J. Qiu, et al., Adv. Sci. 11 (2024) 2305012.
[5] M.R. Kuram, M. Bhanuchandra, A.K. Sahoo, Angew. Chem. Int. Ed. 52 (2013) 4607–4612.
[6] A.Le Roch, M. Hébert, A. Gagnon, Eur. J. Org. Chem. 2020 (2020) 5363–5367.
[7] R.M. Gay, F. Manarin, C.C. Schneider, et al., J. Org. Chem. 75 (2010) 5701–5706.
[8] L. Wu, L. Li, H. Zhang, et al., Org. Lett. 23 (2021) 3844–3849.
[9] X.S. Ji, H.D. Zuo, Y.T. Shen, et al., Chem. Commun. 58 (2022) 10420–10423.
[10] D. Yue, T. Yao, R.C. Larock, J. Org. Chem. 70 (2005) 10292–10296.
[11] S. Zhang, L.M. De Leon Rodriguez, F.F. Li, M.A. Brimble, Chem. Sci. 14 (2023) 7782–7817.
[12] D. Alvarez Dorta, D. Deniaud, M. Mével, S.G. Gouin, Chem. Eur. J 26 (2020) 14257–14269.
[13] W. Ding, S. Wang, J. Gu, L. Yu, Chin. Chem. Lett. 34 (2023) 108043.
[14] J. Gu, J. Gu, L. Yu, Chin. Chem. Lett. 36 (2025) 110727.
[15] A.S. Mackay, J.W.C. Maxwell, M.J. Bedding, et al., Angew. Chem. Int. Ed. 62 (2023) e202313037.
[16] T. Mintz, N.Y. More, E. Gaster, D. Pappo, J. Org. Chem. 86 (2021) 18164–18178.
[17] T. Yamada, Org. Lett. 26 (2024) 5358–5363.
[18] S.N.S. Vasconcelos, I.M. de Oliveira, A. Shamim, et al., Adv. Synth. Catal. 361 (2019) 4243–4254.
[19] P. Wang, Y. Cheng, C. Wu, et al., Chem. Commun. 57 (2021) 12968–12971.
[20] M. Horikawa, S.T. Joy, L.S. Sharninghausen, et al., Chem. Sci. 14 (2023) 12068–12072.
[21] Q.L. Hu, K.Q. Hou, J. Li, et al., Chem. Sci. 11 (2020) 6070–6074.
[22] M. San Segundo, A. Correa, Chem. Sci. 11 (2020) 11531–11538.
[23] I. Urruzuno, P. Andrade-Sampedro, A. Correa, Org. Lett. 23 (2021) 7279–7284.
[24] J. Duan, Y.F. Du, X. Pang, X.Z. Shu, Chem. Sci. 10 (2019) 8706–8712.
[25] R.B. Bedford, M.F. Haddow, R.L. Webster, C.J. Mitchell, Org. Biomol. Chem. 7 (2009) 3119.
[26] N.D. Kharat, C.K. Mahesha, K. Bajaj, R. Sakhuja, Org. Lett. 24 (2022) 6857–6862.
[27] S. Sato, H. Nakamura, Angew. Chem. Int. Ed. 52 (2013) 8681–8684.
[28] A. Schischko, N. Kaplaneris, T. Rogge, et al., Nat. Commun. 10 (2019) 3553.
[29] C. Girón-Elola, I. Sasiain, R. Sánchez-Fernández, E. Pazos, A. Correa, Org. Lett. 25 (2023) 4383–4387.
[30] P. Wang, Y. Cheng, C. Wu, et al., Org. Lett. 23 (2021) 4137–4141.
[31] T. Long, L. Liu, Y. Tao, et al., Angew. Chem. Int. Ed. 60 (2021) 13414–13422.
[32] N. Ichiishi, J.P. Caldwell, M. Lin, et al., Chem. Sci. 9 (2018) 4168–4175.
[33] M. Zhang, P. He, Y. Li, Chem. Sci. 14 (2023) 9418–9426.
[34] K. Osaka, A. Usami, T. Iwasaki, et al., J. Org. Chem. 84 (2019) 9480–9488.
[35] N.E.S. Tay, D.A. Nicewicz, J. Am. Chem. Soc. 139 (2017) 16100–16104.
[36] Y. Yu, L.K. Zhang, A.V. Buevich, et al., J. Am. Chem. Soc. 140 (2018) 6797–6800.
[37] B.X. Li, D.K. Kim, S. Bloom, et al., Nat. Chem. 13 (2021) 902–908.
[38] X. Hou, N. Kaplaneris, B. Yuan, et al., Chem. Sci. 13 (2022) 3461–3467.
[39] C. Song, K. Liu, Z. Wang, et al., Chem. Sci. 10 (2019) 7982–7987.
[40] M. Stangier, A.M. Messinis, J.C.A. Oliveira, H. Yu, L. Ackermann, Nat. Commun. 12 (2021) 4736.
[41] S. Jiang, L. Xiao, L. Pan, et al., Org. Chem. Front. 11 (2024) 1090–1096.
[42] S. You, R. Wang, C. Ma, et al., Org. Chem. Front. 10 (2023) 4606–4615.
[43] N. Declas, J.R.J. Maynard, L. Menin, et al., Chem. Sci. 13 (2022) 12808–12817.
[44] Y. Weng, X. Xu, H. Chen, Y. Zhang, X. Zhuo, Angew. Chem. Int. Ed. 61 (2022) e202206308.
[45] Y. Li, H. Wang, H. Zhang, A. Lei, Chin. J. Chem. 39 (2021) 3023–3028.
[46] A.S. Mackay, R.J. Payne, L.R. Malins, J. Am. Chem. Soc. 144 (2022) 23–41.
[47] H. Cao, R. Wang, Q. Zhang, et al., Org. Chem. Front. 11 (2024) 2566–2571.
[48] C. Kingston, M.D. Palkowitz, Y. Takahira, et al., Acc. Chem. Res. 53 (2020) 72–83.
[49] C. Ma, J.F. Guo, S.S. Xu, T.S. Mei, Acc. Chem. Res. 58 (2025) 399–414.
[50] J.C. Siu, N. Fu, S. Lin, Acc. Chem. Res. 53 (2020) 547–560.
[51] P. Xiong, H.C. Xu, Acc. Chem. Res. 58 (2025) 299–311.
[52] X. Cheng, A. Lei, T.S. Mei, et al., CCS Chem. 4 (2022) 1120–1152.
[53] F. Bu, Y. Deng, J. Xu, et al., Nature 634 (2024) 592–599.
[54] J. Wang, S. Wang, Z. Wei, et al., Science 386 (2024) 776–782.
[55] X. Hu, C. Zheng, X. Song, et al., Adv. Sci. 12 (2025) 2502711.
[56] X. Fang, X. Hu, Q.X. Li, S.F. Ni, Z. Ruan, Angew. Chem. Int. Ed. 64 (2025) e202418277.
[57] Z. Ruan, X. Hu, Y. Huang, X. Fang, Chin. J. Org. Chem. 44 (2024) 903–926.
[58] X. Fang, Y. Zeng, Y. Huang, et al., Nat. Commun. 15 (2024) 5181.